Current European flood-rich period exceptional compared with past 500~years

1Submitted 24 November, 2019. Revision 18 April, 2020

2Current flood-rich period exceptional compared to past 500 3years in Europe

4Günter Blöschl[1†*], Andrea Kiss [1†], Alberto Viglione[1†], …

5

Günter Blöschl	Institute of Hydraulic Engineering and Water Resources Management, Vienna University of Technology, Vienna, Austria
Andrea Kiss	Institute of Hydraulic Engineering and Water Resources Management, Vienna University of Technology, Vienna, Austria
Alberto Viglione	Department of Environment, Land and Infrastructure Engineering (DIATI), Politecnico di Torino, Turin, Italy
Mariano Barriendos	Department of History and Archaeology, University of Barcelona, Barcelona, Spain
Oliver Böhm	Institute of Geography, University of Augsburg, Augsburg, Germany
Rudolf Brázdil	Institute of Geography, Masaryk University, Brno, and Global Change Research Institute, Czech Academy of Sciences, Brno, Czech Republic
Denis Coeur	ACTHYS-Diffusion, Grenoble, France
Gaston Demarée	Royal Meteorological Institute of Belgium, Brussels, Belgium
Maria Carmen Llasat	Department of Applied Physics, University of Barcelona, Barcelona, Spain
Neil Macdonald	Department of Geography and Planning, School of Environmental Sciences, University of Liverpool, Liverpool, United Kingdom
Dag Retsö	Department of Economic History and International Relations, Stockholm University, Stockholm, Sweden
Lars Roald	Norwegian Water Resources and Energy Directorate, Oslo, Norway
Petra Schmocker-Fackel	Department of Hydrology, Federal Office for the Environment (BAFU), Zürich, Switzerland
Inês Amorim	Department of History, Political and International Studies, University of Porto, Porto, Portugal
Monika Bělinová	Global Change Research Institute, Czech Academy of Sciences, Brno, Czech Republic
Gerardo Benito	Department of Geology, National Museum of Natural Sciences, CSIC, Madrid, Spain
Chiara Bertolin	Department of Mechanical and Industrial Engineering, Norwegian University of Science and Technology, Trondheim, Norway
Dario Camuffo	National Research Council, Institute of Atmospheric Sciences and Climate, Padua, Italy
Daniel Cornel	VRVis Research Center for Virtual Reality and Visualization, Vienna, Austria
Radosław Doktor	Centre for Flood and Drought Modelling, Institute of Meteorology and Water Management – National Research Institute, Warsaw, Poland
Líbor Elleder	Czech Hydrometeorological Institute, Prague, Czech Republic
Silvia Enzi	Kleio Studio Associate Research Company, Padova, Italy
João Carlos Garcia	Faculty of Arts, University of Porto, Porto, Portugal
Rüdiger Glaser	Department of Physical Geography, Institute of Environmental Social Sciences and Geography, University of Freiburg, Freiburg, Germany
Julia Hall	Institute of Hydraulic Engineering and Water Resources Management, Vienna University of Technology, Vienna, Austria
Klaus Haslinger	Climate Research Department, Central Institute of Meteorology and Geodynamics (ZAMG), Vienna, Austria
Michael Hofstätter	Climate Research Department, Central Institute of Meteorology and Geodynamics (ZAMG), Vienna, Austria
Jürgen Komma	Institute of Hydraulic Engineering and Water Resources Management, Vienna University of Technology, Vienna, Austria
Danuta Limanówka	Centre for Poland´s Climate Monitoring, Institute of Meteorology and Water Management – National Research Institute, Cracow, Poland

David Lun	Institute of Hydraulic Engineering and Water Resources Management, Vienna University of Technology, Vienna, Austria
Andrei Panin	Institute of Geography RAS, Moscow, Russia & Lomonosov Moscow State University, Moscow, Russia
Juraj Parajka	Institute of Hydraulic Engineering and Water Resources Management, Vienna University of Technology, Vienna, Austria
Hrvoje Petrić	Department of History, Faculty of Humanities and Social Sciences, University of Zagreb, Zagreb, Croatia
Fernando S. Rodrigo	Department of Chemistry and Physics, University of Almería, Spain
Christian Rohr	Department of Economic, Social and Environmental History, Institute of History, University of Bern, Bern, Switzerland
Johannes Schönbein	Department of Physical Geography, Institute of Environmental Social Sciences and Geography University of Freiburg, Freiburg, Germany
Lothar Schulte	Department of Geography, University of Barcelona, Barcelona, Spain
Luís Pedro Silva	Transdisciplinary Research Centre Culture, Space and Memory, University of Porto, Porto, Portugal
Willem H.J. Toonen	Department of Physical Geography, Utrecht University, Utrecht, The Netherlands
Peter Valent	Institute of Hydraulic Engineering and Water Resources Management, Vienna University of Technology, Vienna, Austria
Jürgen Waser	VRVis Research Center for Virtual Reality and Visualization, Vienna, Austria
Oliver Wetter	Department of Economic, Social and Environmental History Institute of History, University of Bern, Bern, Switzerland

† These authors contributed equally to this work.

* e-mail: bloeschl@hydro.tuwien.ac.at

ABSTRACT

There are concerns that recent climate change is altering the frequency and magnitudes of river floods in an unprecedented way[1]. Historical studies have identified flood-rich periods in the past half millennium in various regions of Europe[2]. However, because of the low temporal resolution of existing data sets and the relatively low number of series across Europe, it has remained unclear whether Europe is currently in a flood-rich period from a long term perspective. We analyze how recent decades compare with the flood history of Europe, using a new database composed of more than 100 high-resolution (sub-annual) historical flood series based on documentary evidence covering all major regions of Europe. Here we show that the past three decades were among the most flood-rich periods in Europe in the last 500 years, and that this period differs from other flood-rich periods in terms of its extent, air temperatures and flood seasonality. We identified nine flood-rich periods and associated regions. Among the periods richest in floods are 1560-1580 (Western and Central Europe), 1760-1800 (most of Europe), 1840-1870 (Western and Southern Europe), and 1990-2016 (Western and Central Europe). In most parts of Europe previous flood-rich periods occurred during cooler than usual phases, however the current flood-rich period has been much warmer. In the past, the dominant flood seasons in flood-rich periods were similar to those during the intervening (interflood) periods, but flood seasonality is more pronounced in the recent period. For example, during previous flood and interflood periods, 41% and 42% of Central European floods occurred in summer respectively, compared to 55% of floods in the recent period. The uniqueness of the present-day flood-rich period calls for process-based flood risk assessment tools and flood risk management strategies that account for these changes.

MAIN TEXT

Historical flood context

In recent decades numerous devastating floods have occurred in Europe with enormous economic damage[3]. Flood data over the past 50 years suggest that some parts of Europe are experiencing upward flood trends[4], but it is unclear whether we are currently in a flood-rich period (more frequent and bigger floods than usual in extent and/or magnitude) and, if so, how unusual it is relative to other flood-rich periods during the past 500 years. An exceptional flood-rich period in recent decades would require more intensive and perhaps different adaption measures than a less unusual period. To understand whether recent decades are indeed exceptional, one needs to identify flood-rich periods and their characteristics in past centuries and compare them with recent decades.

The existence of flood-rich periods in the last 500 years has been demonstrated for a number of individual catchments in Europe based on historical documentary evidence[5, 6, 7, 8] and mountain lake sediments[9]. One of the few available regional studies (19 documentary-based data series) identified 1540-1600, 1640-1700, 1730-1790 and 1790-1840 as flood-rich periods in Central Europe[2], which is roughly consistent with sedimentary evidence from a set of Alpine lakes[10] and six floodplains[11] in Central Europe. Several authors have suggested that more frequent flooding in the Little Ice Age (1300-1870), and specifically the late Maunder Solar Minimum (1675-1725), can be related to lower air temperatures[6, 2, 12, 8], but a more universal relationship with air temperatures for other flood-rich periods has not been identified[7, 13, 11]. Temperature anomalies can be considered a proxy for changes in the atmospheric circulation system and are therefore of relevance for assessing past and future flood frequency changes.

Here we analyse the most comprehensive data set of 103 sub-annual flood series over the past 500 years covering all regions of Europe (Extended Data Fig. 1) in order to examine the existence and characteristics of flood-rich periods.

Reconstructing historical flood frequency

The flood series are based upon the collation of published and unpublished series based on chronicles, annals, administrative and legal records, newspapers, and private and official correspondence (Extended Data Table 1). We almost exclusively used contemporary documentation (i.e. written shortly after the flood events) because of its higher reliability relative to non-contemporary documentation. The documentation included direct indicators, such as the level and spatial extent of flood waters relative to identifiable landmarks and, to a lesser extent, indirect indicators such as their environmental or socio-economic impact. For each piece of evidence, a critical, historical source evaluation was conducted, utilizing the local socio-economic and environmental history knowledge of the analysts, in order to minimise errors in dating, interpretation and other possible mistakes originating from social biases.

For 103 river reaches across Europe the documentary evidence on individual floods was transformed into a three-scaled intensity index for the period 1500-2016. The total number of floods contained in the data set are 9576, of which 8954 have a season assigned. In order to account for differences in the representativeness of different series in space, we assigned to each series a representativeness index, which reflects the level of confidence that important floods have been captured. In order to account for temporal observational biases, we assigned each year of each series a rank on a bias index that reflects the completeness of the source material in a historical context. While there is inevitable subjectivity in assigning these indexes, decisions are nonetheless made on the basis of expert judgment of the sources and phenomena in question.

The intensity indices of the series were spatially-temporally interpolated, accounting where possible for uncertainty and bias (see methods section), which resulted in a three dimensional matrix of flood

3

intensities over Europe in the last 500 years with voxel size of 41km*48km*4yrs. This matrix was used to identify contiguous flood-rich periods in space and time by applying an algorithm that connects neighbouring voxels that exceed an intensity threshold. We ranked these flood-rich periods by the sum of the scaled space-time extent and the scaled mean flood intensity. Based on a 500-year Central European air temperature reconstruction[14], which we consider to currently be the highest quality multi-centennial reconstruction in Europe and to be spatially representative (see method section), we compared the average air temperatures of these flood-rich periods with those of the interflood periods before and after. Additionally, we analysed the seasonality of flood occurrence in the flood-rich and interflood periods.

Flood-rich periods in past 500 years

Here we find that the past three decades were among the most flood-rich in Europe during the last 500 years, and that this period differs from other flood-rich periods in terms of its extent, associated air temperatures and flood seasonality.

The nine flood-rich periods identified are rather regularly distributed in time, but the latest 30 year period is separated from the past periods by a 90-year disaster gap in most of Europe with the occurrence of few floods (Fig. 1, Table 1, Fig. 2) in line with historical flood impact research[15]. The most highly ranked flood-rich periods, on the basis of their space-time extent and flood intensity, were 1560-1580 (period II in Western and Central Europe), 1760-1800 (period V in most of Europe), 1840-1870 (period VI in Western and Southern Europe), and 1990-2016 (period IX in Western and Central Europe) (Table 1, Video 1).

Individually, the nine flood-rich periods cover only part of Europe with areas between 0.41 and 1.83 10^6 km² (Extended Data Table 2), out of a total land area of xx 10^6 km² examined. There is a tendency for flood-rich periods to occur more often in Central and Western Europe than in other regions (Fig. 1, Fig. 3).

The most recent flood-rich period is 1990-2016, the second largest in spatial extent (1.77 10^6 km²) and the third largest in spatio-temporal extent (18.7 10^6 km².yrs), indicating that it not only covered a large part of Europe, but also a significant duration in time (Extended Data Table 2). 2016 is the end of the data and possibly not the end of this flood-rich period.

The average air temperatures in most Central European flood-rich periods were around 0.3°C lower than those in the intervals between flood-rich periods (termed interflood periods) (Fig. 4). Flood-rich period II was particularly cold and is known for the great glacier advances in the Alps[16]. The confidence bounds of the temperatures in most flood-rich periods of the past vs the interflood periods in Fig. 4b are below the 1:1 line, indicating that the differences are statistically significant. The only exception was period IV (1630-1660), with average annual temperature similar to those of the interflood periods, resulting from warm summers, however autumns and winters when most of the floods occurred were notably colder than usual[17]. This is consistent with the other flood-rich periods that were colder overall than the interflood periods. In other parts of Europe, there is also a tendency for flood-rich periods I to VIII to be colder than the interflood periods, with differences of about 0.3°C and 0.2°C in Western and Southern Europe, respectively (Extended Data Fig. 4).

While flood-rich periods in the past have thus mostly been associated with comparatively colder air temperatures, this is not the case for the most recent flood-rich period IX, which was on average about 1.4°C warmer than the previous interflood period in all regions.

The time of year when floods most often occur differs between regions and periods (Fig. 5, Extended Data Table 1). In Central Europe, floods mainly occur in summer. In the Central European flood-rich and the interflood periods of the past, 41% and 42% of the floods occurred in summer, respectively. In contrast, during the recent flood period IX, 55% of the floods occurred in summer. The red

confidence bounds in Fig. 5b do not overlap, indicating that the differences in summer flood frequencies between the recent flood period IX and the previous periods are significant and have not simply occurred by chance. In Southern Europe, the corresponding frequencies for floods in autumn (which is the dominant flood season) increased from 43% (flood rich) and 41% (interflood) to 54% (flood period IX), and in Western Europe, the corresponding frequencies for floods in winter (which is the dominant flood season) increased from 49% (flood rich) and 46% (interflood), to 55% (flood period IX) (Extended Data Fig. 5).

Flood processes and implications

While there is some overlap between flood-rich periods detected here and those found previously in Central Europe based on 19 series[2] (their periods 1540-1600, 1640-1700, 1730-1790 approximately match periods II, IV and V here), their last period 1790-1840 does not emerge as a flood-rich period here. Similarly, the Late Maunder low solar intensity period (1675-1725) sometimes associated with flood occurrence in Europe[6] was not particularly flood rich on a European level. The extent of the recent flood-rich period IX is consistent with the increasing trends in flood discharges observed in Northwestern and Central Europe in recent decades[4].

Previous analyses did not find coherent flood-temperature relationships at a European scale[6, 7, 8], which may partly reflect the low number of high-resolution series. At a local to regional scale (e.g. Bohemia, Eastern Spain) and in some periods (e.g. late Maunder Solar Minimum and 18th-19th century) flood-temperature associations were demonstrated[6, 18]. Our new comprehensive flood data set provides clear evidence that such a relationship exists across Europe over the past 500 years.

The most significant flood-rich period in our ranking, Period V (1760-1800), occurred during the decades preceding the French Revolution. Notably lower temperatures also prevailed during this period. Air pressure reconstructions[19] suggest that there was frequent polar air intrusion into North America, the North Atlantic region and Western Europe associated with an expanded polar cell, and lower north-south air pressure gradients (negative Northern Atlantic Oscillation (NAO) index) pointing towards frequent blocking situations in Europe[20, 21]. In the 1780s, the sea ice extent around Iceland was at its greatest during the last 500 years[22]. The 1783 Lakigigar volcanic eruption in Iceland may have further contributed to lowering the temperatures[23].

Temperature is the most easily observed and most predictable parameter of a changing climate system. Whilst flood-producing precipitation is not necessarily driven by air temperature anomalies, both are controlled by large-scale atmospheric circulations and ocean interactions[24]. In summer, the relationship between temperature and precipitation tends to be negative, as precipitation associated with cyclones implies more cloud cover and less solar radiation (Gagen et al. 2016)[25]. In winter, in contrast, there is a tendency for cyclones to transport moist and relatively warm air masses from the Atlantic to Europe resulting in a positive relationship[26]. Spatio-temporal variations of precipitation and flooding depend on the NAO because of the link between NAO and the position of Atlantic storm tracks[27, 28, 24]. In winter, enhanced cyclone activity occurs in Northern Europe during positive NAO phases while in Southern Europe this is the case during negative NAO phases[29], as the position of Atlantic storm tracks migrate northward and southward, respectively. The decadal oscillations of the storm track position also lead to subcontinental temperature variations through the redistribution of cloud cover and precipitation as a result of internal climate variability[25, 30]. The exact mix of influences driving the past flood-rich periods remains an open question that will require further work. Also, we used a Central European air temperature reconstruction here and future work should incorporate further regionally specific reconstructions once available for the past 500 years.

Another factor contributing to higher floods in cold periods is soil moisture. Lower temperatures lead to less evaporation and hence higher soil moisture which, in turn, results in larger floods, for the same rainfall[31, 32]. The June 2013 flood in Central Europe is an example of this. The preceding

winter and spring were cold, soil moisture was much higher than usual and thus the flood was much larger than floods with dry antecedent soils[33]. While the temperature-precipitation relationship in Europe depends on the season, annual rather than seasonal temperatures are analysed here so that not only flood event properties but also antecedent soil moisture and snow conditions are considered, which can be relevant for flood magnitudes over multiple-seasons.

During the past 30 years, hydroclimatic conditions over Europe have shifted to their millennial boundaries with a dry anomaly in Southern-, and a wet anomaly in Central and Northern Europe[34]. These changes appear to be caused by a persistent anomalous circulation regime of frequent low pressure systems over the East Atlantic and Western Europe[34]. Observational data suggest this pattern to be associated with a warm sea surface temperature anomaly in the Northern Atlantic Ocean[35, 34], positive Atlantic Multidecadal Oscillation (AMO) and negative NAO, resulting in conditions that are likely to cause heavy precipitation through intense cyclone development and frequent blocking over Western and Central Europe[36, 37, 38]. Although contemporary air temperatures are much higher, there are similarities to the atmospheric circulation regime that prevailed in Period V (1760-1800). However, climate model simulations suggest that present and future precipitation increases in Europe may be driven more by thermodynamics, i.e. the higher water-holding capacity of a warmer atmosphere, than by changes in circulation[39, 30]; with increased evaporation and shallower snow packs also modulating floods[4]. It is therefore not clear how long the current flood-rich period IX will continue into the future.

Systematic records have demonstrated that the timing of river floods in Europe has changed since 1960[40]. Fig. 5 and Extended Data Fig. 5 demonstrate, however, that a change towards more frequent summer floods in Central Europe, more frequent winter floods in Western and more frequent autumn floods in Southern Europe started earlier than this, around 1940. The finding of increasing flood occurrence in the dominant flood season in all regions of Europe since 1960 in this paper is consistent with trends in flood timing and associated flood generating processes, such as earlier snowmelt and fewer ice jam floods in Central Europe, and a seasonal shift of winter storms in the Atlantic region of Europe[2, 4, 40, 41, 42]. In the Mediterranean, the enhanced evaporation and convective activity have increased the frequency of autumn floods[4, 43, 44].

In a global context, the European analysis presented here is the first, large-scale, high-resolution identification of flood-rich periods over multiple centuries. In other continents, flood-rich periods have been identified more locally. For example, in the states of Tabasco and Chiapas, Mexico, floods clustered during 1650-1680 and 1920-1950[45], which indicates some overlap with northern Europe (Fig. 2). At the River Paraná in South-America the 1590s, 1620s, 1740s and 1770s were flood-rich[46], but they were mainly due to El-Niño events, so one would expect different causal mechanisms from Europe. In Asia, millennial-scale investigations suggest larger floods occurred between 1500 and 1700 on the River Yangtze[47].

Our research advances the global study of flood sensitivity to climate variability. Eventually, it may be possible to draw correlations between flood-rich periods across the globe that go beyond individual river basins and flood events. While flood management is currently strongly based on the analysis of systematic data in past decades, extending the time window to past centuries would vastly strengthen the analysis, as they may provide a more complete guide to possible future flood changes thereby allowing the creation of predictive tools that can enhance adaptation capacity at global and local scales. We have strongly shown the potential of documentary data to contribute to such work. The finding that the most recent 30 years are separated from past flood-rich periods by a 90 year disaster gap in most of Europe may explain why both public and flood managers have been surprised by the recent floods[48]. Flood risk assessment tools and flood risk management strategies need to account for the fact that we are currently in an exceptional flood-rich period in terms of timing of flood occurrence, magnitudes and spatial extent within Europe. Process-based models that capture the physical mechanisms in the atmosphere and rainfall-runoff transformation on the land surface, including the role of precipitation, soil moisture, snowmelt and seasonality in flood

generation in both recent and historical times, will be an essential component of flood-risk assessment tools in a changing climate.

References

[1] IPCC. Managing the Risks of Extreme Events and Disasters to Advance Climate Change Adaptation. A Special Report of Working Groups I and II of the Intergovernmental Panel on Climate Change. (Cambridge University Press, Cambridge, UK and New York, NY, USA, 2012).

[2] Glaser, R. et al. The variability of European floods since AD 1500. *Clim. Change* **101**, 235–256 (2010).

[3] UNDRR, Global Assessment Report on Disaster Risk Reduction (Geneva Switzerland, 2019).

[4] Blöschl, G. et al. Changing climate both increases and decreases European river floods. *Nature* **573**, 108–111 (2019).

[5] Camuffo, D., & Enzi, S. The analysis of two bi-millenary series: Tiber and Po river floods. In: *Climatic variations and forcing mechanisms of the last 2000 years* (eds Jones, P., Bradley, R. & Jouzel, J.) (Heidelberg Springer, 1996).

[6] Brázdil, R. et al. Fluctuations of floods if the River Morava (Czech Republic) in the 1691-2009 period: Interactions of natural and anthropogenic factors. *Hydrolog. Sci. J.* **56**, 467–485 (2011).

[7] Schmocker-Fackel, P. & Naef, F. Changes in flood frequencies in Switzerland since 1500. *Hydrol. Earth Syst. Sci.* **14**, 1581–1594 (2010).

[8] Pichard, G., Arnaud-Fassetta, G., Moron, V., & Roucaute, E. Hydro-climatology of the Lower Rhône Valley: historical flood reconstruction (AD 1300-2000) based on documentary and instrumental sources. *Hydrolog. Sci. J.* **62**, 1772–1795 (2017).

[9] Wilhelm, B., Vogel, H., Crouzet, C., Etienne, D., & Anselmetti, F.S. Frequency and intensity of palaeofloods at the interface of Atlantic and Mediterranean climate domains. *Clim. Past* **12**, 299–316 (2016).

[10] Wirth, S.B., Glur, L., Gilli, A. & Anselmetti, F.S. Holocene flood frequency across the Central Alps – solar forcing and evidence for variations in North Atlantic atmospheric circulation. *Quat. Sci. Rev.* **80**, 112–128 (2013).

[11] Schulte, L., Wetter, O., Wilhelm, B., Peña, J.C., Amann, B., Wirth, S.B., Carvalho, F., & Gómez-Bolea. Integration of multi-archive datasets for the development of a four-dimensional paleoflood model of alpine catchments. *Glob. Planet. Change* **180**, 66–88 (2019).

[12] Retsö, D. Documentary evidence of historical floods and extreme rainfall events in Sweden 1400-1800. *Hydrol. Earth Syst. Sci.* **19**, 1307–1323 (2015).

[13] Glur, L. et al. Frequent floods in the European Alps coincide with cooler periods of the past 2500 years. *Nat. Sci. Rep.* **3**, 2770 (2013).

[14] Dobrovolný, P. et al. Monthly and seasonal temperature reconstructions for Central Europe derived from documentary evidence and instrumental records since AD 1500. *Clim. Change* **101**, 69–107 (2010).

[15] Pfister, C. The “Disaster Gap” of the 20th century and the loss of traditional disaster memory (in German). *Gaia* **18**, 239–246 (2009).

[16] Nicolussi, K., Joerin, U.E., Kaiser, K.F., Patzelt, G. & Thurner, A. Precisely dated glacier fluctuations in the Alps over the last four millennia Part 3. In: Global Change in Mountain Regions. (ed Price, M.F.) (Duncow Sapiens, 2006), 59-60.

[17] Glaser, R. *Klimageschichte Mitteleuropas: 1200 Jahre Wetter, Klima, Katastrophen* (Darmstadt Primus Verlag, 2013), 94.

[18] Barriendos, M. & Martin-Vide, J. 1998. Secular climatic oscillations as indicated by catastrophic floods in the Spanish Mediterranean coastal area (14th-19th centuries). *Clim. Change* **38**, 473–491 (1998).

[19] McNally, L. K. Reconstruction of late 18th century upper-air circulation using forensic synoptic analysis. *Hist. Meteor.* **2**, 105-122 (2005).

[20] Cornes, R.C., Jones P.D., Briffa, K.R. & Osborn, T.J. Estimates of the North Atlantic Oscillation back to 1692 using a Paris–London westerly index. *Int. J. Climatol.* **33**, 228–248 (2013).

[21] Slonosky, V.C., Jones, P.D. & Davies, T.D. Variability of the surface atmospheric circulation over Europe, 1774-1995. *Int. J. Climatol.* **20**, 1875–1897 (2000).

[22] Ogilvie, A.E.J. Documentary evidence for changes in the climate of Iceland, A.D. 1500 to 1800. In: Climate Since A.D. 1500 (eds Bradley, R.S. & Jones, P.D.) (London Routledge, 1992), 92–117.

[23] Brázdil, R., et al. European floods of the winter 1783/84: scenarios of an extreme event during the 'Little Ice Age.' *Theor. Appl. Climatol.* **100**, 163–189 (2010).

[24] Woollings, T., Hannachi, A. & Hoskins, B. Variability of the North Atlantic eddy-driven jet stream. *Q. J. R. Meteorol. Soc.* **136**, 856–868 (2010).

[25] Gagen, M. et al. North Atlantic summer storm tracks over Europe dominated by internal variability over the past millennium. *Nat. Geosci.* **9**, 630–635 (2016).

[26] Hurrell, J.W. & Van Loon, H. Decadal variations in climate associated with the North Atlantic Oscillation. In Diaz, H.F., Beniston, M. & Bradley, R.S. Climatic change at high elevation sites. (Dordrecht Springer, 1997), 69–94.

[27] Nobre, G. G., Jongman, B., Aerts, J. C. J. H., & Ward, P. J. The role of climate variability in extreme floods in Europe. *Env. Res. Lett.* **12**, 084012 (2017).

[28] Steirou, E., Gerlitz, L., Apel, H., Sun, X & Merz, B. Climate influences on flood probabilities across Europe. *Hydrol. Earth Syst. Sci.*, 23, 1305–1322 (2019).

[29] Folland, C. K., Knight, J., Linderholm, H. W., Fereday, D., Ineson, S., & Hurrell, J. W. The summer North Atlantic Oscillation: past, present, and future. *J. Clim.* **22**, 1082–1103 (2009).

[30] Raible, C., Messmer, M. B., Lehner, F., Stocker, T., & Blender, R. Extratropical cyclone statistics during the last millennium and the 21st century. *Clim. Past* **14**, 1499–1514 (2018).

[31] Komma, J., Blöschl, G. & Reszler, C. Soil moisture updating by Ensemble Kalman Filtering in real-time flood forecasting. *J. Hydrol.* **357**, 228–242 (2008).

[32] Grillakis, M.G. et al. Initial soil moisture effects on flash flood generation – A comparison between basins of contrasting hydro-climatic conditions. *J. Hydrol.* **541**, 206–217 (2016).

[33] Blöschl, G., Nester, T., Komma, J., Parajka, J. & Perdigao, R.A.P. The June 2013 flood in the Upper Danube Basin, and comparisons with the 2002, 1954 and 1899 floods. *Hydrol. Earth Syst. Sci.* **17**, 5197–5212 (2013).

[34] Markonis, Y., Hanel, M., Máca, P., Kyselý, J., & Cook, E.R. Persistent multi-scale fluctuations shift European hydroclimate to its millennial boundaries. *Nat. Commun.* **9**, 1767 (2018).

[35] Sutton, R.T. & Dong, B. Atlantic Ocean influence on a shift in European climate in the 1990s. *Nat. Geosci.* **5**, 788–792 (2012).

[36] Hofstätter, M. & Blöschl, G. Vb Cyclones Synchronized with the Arctic/North Atlantic Oscillation. *J. Geophys. Res. D* **124**, 3259–3278 (2019).

[37] Hofstätter M., Lexer A., Homan M., & Blöschl, G. Large-scale heavy precipitation over central Europe and the role of atmospheric cyclone track types. *Int. J. Clim*. **38**, e497–e517 (2018).

[38] Messmer, M., Gómez-Navarro, J.J., & Raible, C.C. Climatology of Vb cyclones, physical mechanisms and their impact on extreme precipitation over Central Europe. *Earth Syst. Dynam.* **6**, 541–553 (2015).

[39] Hawcroft, M., Walsh, E., Hodges, K. & Zappa, G. Significantly increased extreme precipitation expected in Europe and North America from extratropical cyclones. *Env. Res. Lett.* **13**, 124006 (2018).

[40] Blöschl, G. et al. Changing climate shifts timing of European floods. *Science* **357**, 588–590 (2017).

[41] Berghuis, W.R, Harrigan, S., Molnar, P., Slater, L.J., & Kirchner, J.W. The relative importance of different flood-generating mechanisms across Europe. *Water Resour. Res.* **55**, 4582–4593 (2019).

[42] Xoplaki, E., Gonzalez-Rouco, J. F., Luterbacher, J., & Wanner, H. Wet season Mediterranean precipitation variability: influence of large-scale dynamics and trends. *Clim. Dynam.* **23**, 63–78 (2004).

[43] Barrera-Escoda, A. & Llasat, M. C. (2015) Evolving flood patterns in a Mediterranean region (1301–2012) and climatic factors – the case of Catalonia, *Hydrol. Earth Syst. Sci.*, **19**, 465–483.

[44] Barriendos, M. & Rodrigo, F.S. 2006. Study of historical flood events on Spanish rivers, using documentary data. *Hydrolog. Sci. J.* **51**, 765–783 (2006).

[45] Valdés-Manzanilla, A. Historical floods in Tabasco and Chiapas during sixteenth–twentieth centuries. *Nat. Hazards* **80**, 1563–1577 (2016).

[46] Prieto, M.R. ENSO signals in South America: rains and floods in the Paraná River region during colonial times. *Clim. Change* **83**, 39–54 (2007).

[47] Tong, J., Quiang, Z., Deming, Z., & Yijin, W. Yangtze floods and droughts (China) and teleconnections with ENSO activities (1470-2003). *Quatern. Int.* **144**, 29–37 (2006).

[48] Merz, B., Vorogushyn, S., Lall, U., Viglione, A., & Blöschl, G. Charting unknown waters - On the role of surprise in flood risk assessment and management. *Water Resour. Res.* **51**, 6399–6416 (2015).

ACKNOWLEDGEMENTS

This work was supported by the ERC Advanced Grant 'FloodChange' project (number 291152), the Horizon 2020 ETN 'System Risk' project (number 676027), the DFG project FOR 2416, the FWF projects I 3174 and W1219-N22, projects CGL2016-75475/R, CGL2017-86839-C3-1-R and CGL2016-75996-R, Spanish Ministry of Science, Innovation and Universities, and project CZ.02.1.01/0.0/0.0/16_019/0000797, Ministry of Education, Youth and Sports of the Czech Republic. We acknowledge all flood data providers listed in Extended Data Table 1, and would like to thank Julia Lajus for pointing us to the published Neva series.

AUTHOR CONTRIBUTIONS

G. Blöschl, A.K. and A.V. designed the study and wrote the first draft of the paper. G. Blöschl initiated the study and provided guidance for the analyses. A.K. collated the database with the help of most of the co-authors, and provided guidance for the analyses. A.V. performed all quantitative analyses of the flood data. M. Barriendos, O.B., R.B., D. Coeur, G.D., A.K., M.C.L., N.M., D.R., L.R., P.S., I.A., M. Bělinová, G. Benito, C.B., D. Camuffo, D. Cornel, R.D., L.E., S.E., J.C.G., R.G., D. Limanówka, A. P., H.P., F.S.R., C.R., J.S., L.S., L.P.S., W.H.J.T. and O. W. developed historical river flood series. J.H., K.H., M.H.,

J.K., D. Lun, J.P. and P.V. advised on the data analysis. D. Cornel and J. W. rendered Fig. 1 and the Supplementary Video. All authors interpreted results, and contributed to framing and revising the paper.

Competing financial interests

The authors declare no competing financial interests.

AUTHOR INFORMATION Correspondence should be addressed to

G. B. (bloeschl@hydro.tuwien.ac.at)

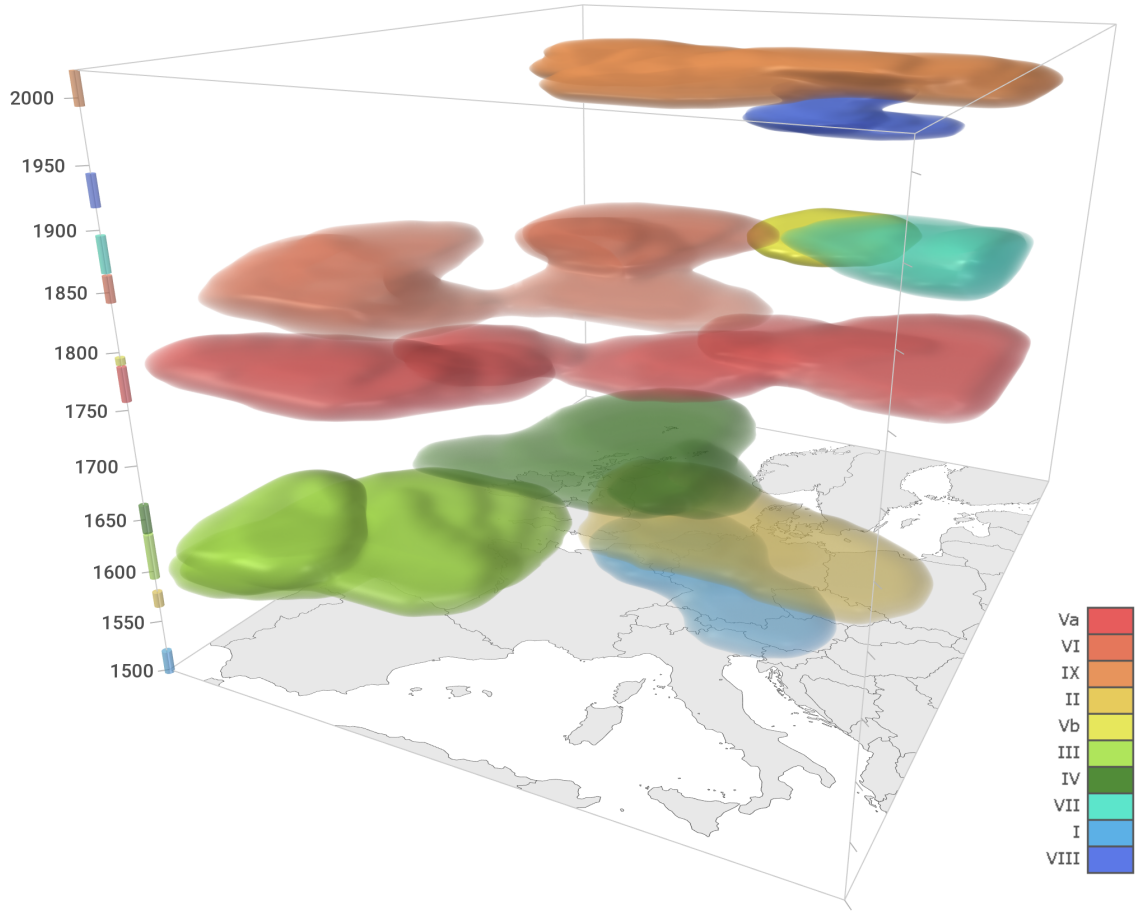

Fig. 1| Flood-rich periods in Europe in the past 500 years. Periods are coloured by their rank, with red (period Va) indicating the strongest and blue (period VIII) indicating the weakest period (Table 1). For a dynamic visualisation see Supplementary Video.

Table 1 Flood-rich periods in Europe since 1500. Regions are defined in the methods section. Rank 1 (period Va) indicates the strongest and rank 10 indicates the weakest period (see Extended Data Fig. 2). Va and Vb were given a combined name due to their overlap in time. * 2016 is the end of the data and possibly not the end of period IX.

Periods	Full time period	Spatial extension (regions)	Rank

10

I	1500-1520	Western Europe, Central Europe	9
II	1560-1580	Western Europe, Central Europe	4
III	1590-1640	Iberia, Southern France	6
IV	1630-1660	Western Europe, West-Central Europe, Northern Italy	7
V	1750-1800	Va Central Europe, Western Europe, Southern Europe Vb Scandinavia	1 5
VI	1840-1880	Western Europe, Southern Europe	2
VII	1860-1900	East Central Europe	8
VIII	1910-1940	Scandinavia	10
IX	1990-2016*	Western Europe, Central Europe, Italy	3

374

375

376

11

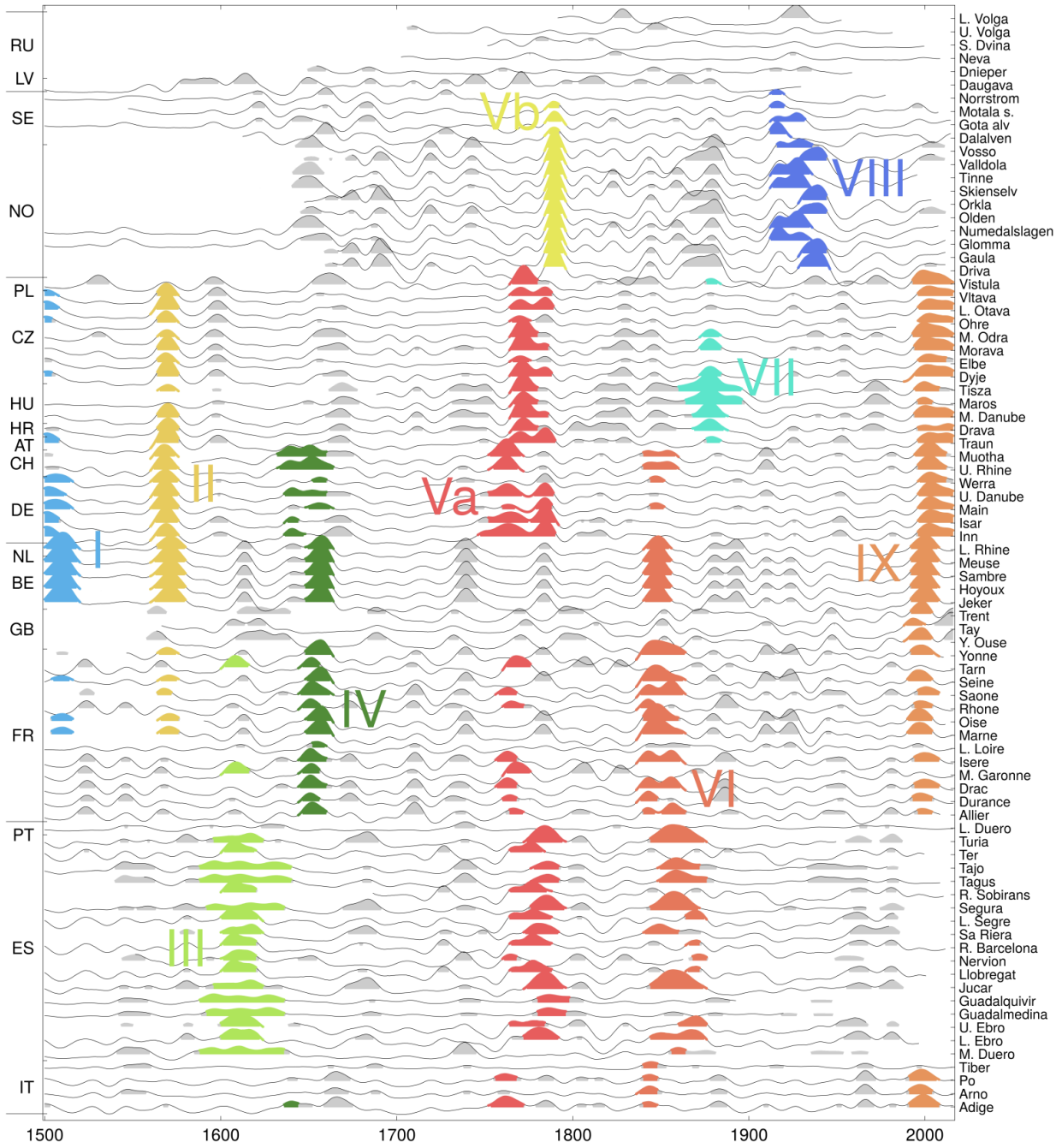

Fig. 2: Flood intensities interpolated in space and time (thin black lines) and flood-rich flood periods identified (coloured areas). For numbers of flood-rich periods see Table 1 and Extended Data Table 2. Grey areas indicate years that exceed the flood intensity threshold and are not in one of the identified flood-rich periods. Countries (left vertical axis) are grouped by region (from top to bottom: Eastern, Northern, Central, Western and Southern Europe).

12

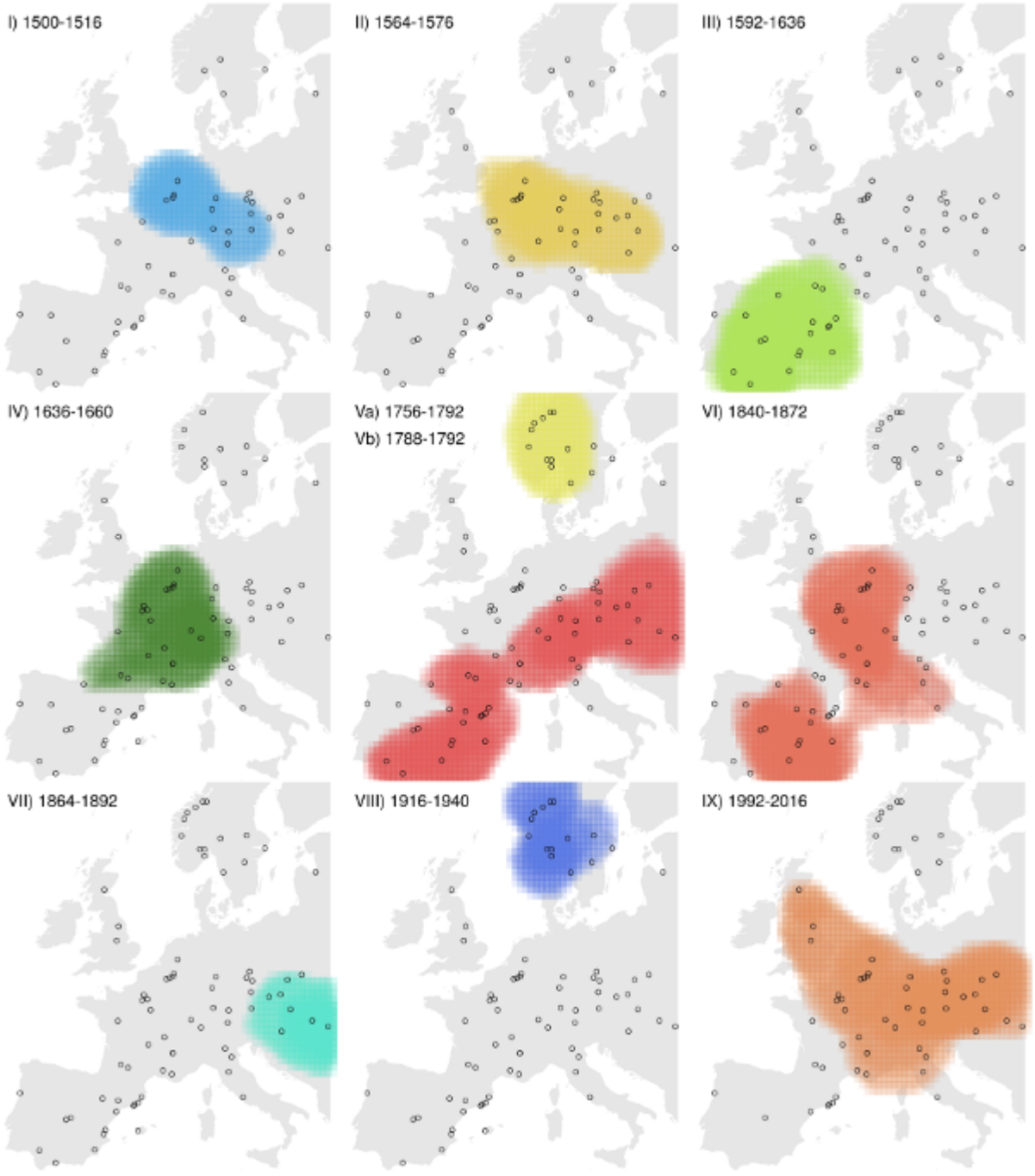

Fig. 3: Flood-rich periods in Europe. For numbers see Table 1 and Extended Data Table 2. Periods are coloured by their rank, with red (period Va) indicating the strongest and blue (period VIII) indicating the weakest period. Also see Extended Data Table 2 for the rank.

13

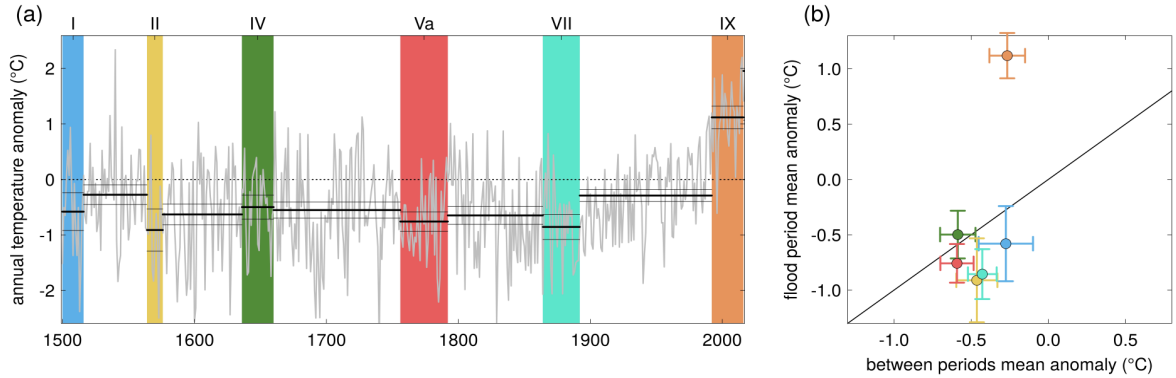

Fig. 4| Anomalies of annual air temperatures from their 1961-1990 mean within and outside flood-rich periods in Central Europe. (a) Time series of air temperature anomalies (grey line) and their averages and 90% confidence bounds (black lines), and flood-rich periods indicated by coloured bars. (b) Relationship between average temperature anomalies in flood-rich periods and those of the intervals in between. Error bars show 90% confidence bounds. Colours correspond to those of the flood-rich periods in (a). Only the flood-rich periods that affected Central Europe are shown here. For other regions see Extended Data Fig. 4.

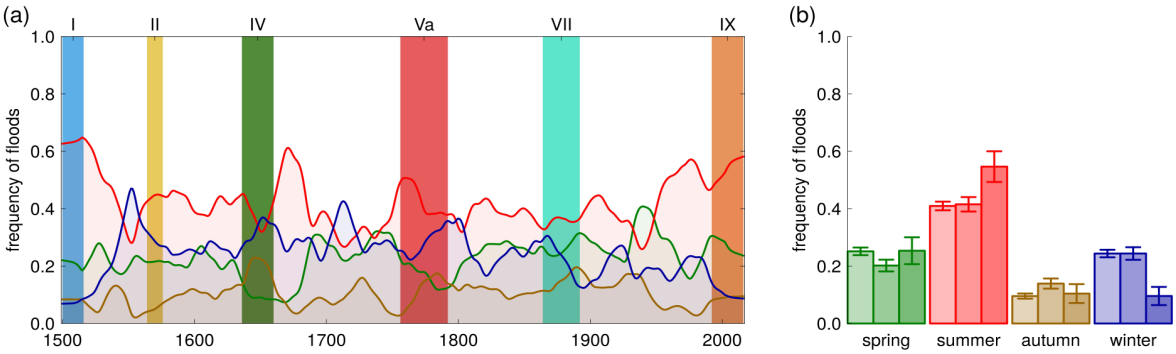

Fig. 5| Seasonality of floods within and outside flood-rich periods in Central Europe. (a) Time series of smoothed frequency of floods in four seasons (lines, green: spring, red: summer, brown: autumn, blue: winter) and flood-rich periods indicated by coloured bars. (b) Frequency of floods in four seasons. Left bars: interflood periods; middle bars: flood-rich periods of the past; right bars: flood-rich period IX (1990-2016). Error bars show 90% confidence bounds.

Methods

Development of historical flood database

The development of the historical flood series from documentary evidence followed standard flood magnitude classification methods. The evidence consisted of historical documentation including narratives (e.g. chronicles), administrative sources, newspapers, and private and official correspondence (e.g. letters). We used almost exclusively (over 90%) contemporary documentation, written shortly after the flood events, rather than non-contemporary documentation, because of its higher reliability[49]. The documentation always included direct indicators, such as the level and spatial extension of flood waters relative to identifiable landmarks and, in most cases, indirect indicators such as the environmental or socio-economic impact that provide complementary information. For each piece of evidence, a critical, historical source evaluation was conducted, utilizing the local

14

socio-economic and historical source knowledge of the analysts, in order to minimise errors in dating, interpretation and other possible mistakes originating from social biases.

Individual series do not necessarily originate from exactly the same location. Series "HU01 Middle Danube" (see Extended Data Table 1), for example, was compiled based on evidence from the Danube reach between Bratislava and Mohács, a reach of about 400 km, as this reach can be considered approximately homogeneous in terms of flood magnitude. Reaches were judged as approximately homogeneous if the sources at different locations along that reach usually suggested the same index value for the same event. In other cases, the information was more focused. For example, series "ES19 Ter" is based on information from Girona only. Coordinates were assigned to each series representing the centre of gravity of the source information. For the series "HU01 Middle Danube", for example, the coordinates were selected at Komárom, which is slightly upstream of the middle of the reach.

The documentary evidence was then transformed into a numerical intensity index. We applied the most widely used three-scaled index method, differentiating flood events into intensities i_f of notable (no. 1), great (no. 2) and extraordinary (no. 3) magnitudes[50, 51, 52]. A flood was considered notable (no. 1) if the flood waters exceed the river banks, but not significantly; great (no. 2) if it they considerably exceed the river banks, often over an extended period of time with local hydromorphological changes; and extraordinary (no. 3) if the flood waters are much higher and spatially more extended than usual floods, often unexpected and with major disruption of daily life. Historical documents would typically refer to these three categories as flood, great flood and very great flood (or extraordinary flood or deluge), respectively[51]. Since the intensity index was mainly based on direct indicators, it is intended to reflect flood magnitudes, rather than flood damage. The index also accounted for the construction of flood protection measures such as levees[18]. For example, at Szeged in Hungary (HU03 Tisza series) a major levee system was constructed in the early 1880s. In the period before, a flood would be considered a notable (no. 1) flood if the lower floodplain around the town, the pastures and some cultivated fields were inundated. In the period after, a flood would be considered a notable (no. 1) flood if water significantly exceeded the quay (low lying road along the shoreline) even though the pastures and the cultivated fields in the lower floodplain were not inundated because they were protected[51]. Similar differentiations were made for no. 2 and no. 3 floods. Land-use change effects were assumed to be small, as 80% of the catchments were larger than 700 km² and land use changes tend only to be important for small catchments[53]. This is because changes in the infiltration capacity of soils mainly affect flood generation resulting from thunderstorms in small catchments[53, 54, 55]. Additionally, for all series we identified (i) years with no floods, (ii) years with probably no floods, (iii) years with either no floods or missing data (i.e. no information) and (iv) years outside the period covered by the series.

In order to account for differences in the representativeness of different series in space, we assigned to each series a representativeness index u (1: low representativeness, 2: average representativeness, 3: high representativeness), that reflects the level of confidence that important floods have been captured, based on a holistic assessment of the completeness of the source material in a regional context. For example, SE02 Motala strom series was considered highly representative (u=3) because there is high confidence that all the important floods have been captured even though total number of reported floods may be lower than in other stations. In this case we have high confidence because of the nature of source type (consistent local chronicles and diaries)[12]. There is also a tendency for series of larger rivers to have higher representativeness than series of smaller rivers because of the higher population density and the more frequent presence of cities.

In order to account for temporal observational biases, we assigned to each year of each series a bias index, on a scale from 1 to 4, that reflects the completeness of the source material in a historical context. Index values from 1 to 4 indicate, respectively, no data, periods with possibly missing data,

average, and periods with overly dense data compared to the average of that series. For example, AT01 Traun for the period 1500-1600 benefitted from the availability of weekly bridge master accounts, which make the data much more complete than later when such accounts were not available[56]. For most series, however, the more recent years are more complete.

A total of 103 river flood series were compiled. Out of these, 70 start in 1500. 82, 99 and 103 series start in or earlier than 1600, 1700 and 1800, respectively (Extended Data Figs. 1-3). The total number of floods contained in the data set are 9576 of which 8954 have a season assigned. The seasons are spring (March - May), summer (June – August), autumn (September – November) and winter (December – February). There are 5696 no. 1 floods (notable), 2616 no. 2 floods (great) and 1264 no. 3 floods (extraordinary).

Interpolation

In interpolating flood intensity in space and time only class 2 and 3 floods are used, since they are considered to be less affected by observation bias. This is because class 2 and 3 floods tend to result in higher disruption of the daily life than class 1 floods, which increases the societal relevance and thus the likelihood of being documented. When a series contained more than one event per year, the intensities of the individual events i_f were aggregated to one annual intensity i_a by $i_a = \sqrt{\sum i_f^2}$ where the summation is over the events of that year. To reduce some of the spatial correlations, only 83 out of the 103 series were used for interpolation, excluding series with similar intensities to neighbouring series either because they are nested catchments or derived from homogeneous flood regions (denoted 'supplementary' in Extended Data Fig. 1). Some spatial correlation may remain which may bias the results of the interpolation.

In order to reduce observation bias, 0 intensities (i_a=0) were added randomly in some of the years when no class 2 or 3 flood was recorded with probability $p_0(t) = 1 - (1 - p_f(t))^{\alpha}$ where the annual flood probability $p_f(t)$ was estimated from the occurrence of no. 2 and 3 floods within a 100-year time window around the target year t. The exponent α was set to 10, based on test simulations. The consistency of the bias reduction method with the bias index (Extended Data Fig. 2) was checked visually by assessing how many zero values were added in periods characterised by different bias indices. In periods with possible missing data and in periods with overly dense data the method added a smaller and larger number of zeroes than average, respectively, suggesting that the bias reduction method is consistent with the bias index. The validity of the bias reduction method was checked by examining whether monotonic trends appeared over the entire 500 year period in the interpolated flood intensities. While, without bias correction, most major events would be identified in the second half of the 500 yr period, with bias correction, the events were more uniformly distributed in time and there were no monotonic trends in line with the historical expert assessment. The bias index was used to test the bias reduction method rather than to modify the flood intensity in each year and station individually, in order to enhance the repeatability and spatial consistency of the analysis.

The intensities i_a were interpolated using the Thin Plate Spline regression algorithm of the *fastTps* function in the R package *fields*. The coordinates of the series were transformed into kilometres by an Azimuthal Equidistant projection centred at 51°N and 7°E. The interpolation is in space and time, so some equivalence of space and time is needed reflecting a typical relationship between the extent and duration of flood-rich periods in Europe. Based on space-time empirical variograms[57] of the intensities i_a and visual examination we chose a ratio of 50 km per year.

The *fastTps* function assigns a weight to each data point that reflects the inverse of its uncertainty. These weights were calculated based on the representativeness index u of each series and the annual flood intensity i_a, as $w=k(u/2)^2$ where k is 0.2, 1.0 and 1.5 for $i_a<1.5$, $1.5<i_a<2.5$ and $i_a>2.5$, respectively. The small weights of the 0 intensities were chosen to reflect their larger uncertainty.

16

The possible drawback of this procedure is an element of subjectivity of the parameters, but the results were more plausible from a historical expert perspective, than when ignoring the differences in representativeness of the series. The smoothing and tapering range parameters of *fastTps* were set to 10 and 20 years (or 1000 km), respectively, based on an expert assessment of test simulations. A linear drift component was selected.

To increase the robustness of the procedure and assess the sensitivity of the results to adding 0 intensities, the space-time interpolation was repeated 50 times with 50 different realisations of 0 intensities. The resulting mean i_i of the interpolated intensities represents a three dimensional matrix of flood intensities i_i over Europe in the last 500 years with voxel size of about 41 km*48 km*4 yrs. This matrix was used for identifying contiguous flood periods in space and time using an algorithm that connects neighbouring voxels that exceed an intensity threshold[58]. We set the threshold i_i^* to the 95% quantile of the interpolated i_i over the matrix (i_i^*=1.375), which means that these contiguous periods collectively cover 5% of the space-time domain. A comparison of the flood-rich periods obtained for different realisations of 0 intensities showed some differences, but the main pattern remained. For example, the top ranked periods always remained at the top with similar spatial and temporal extents.

We calculated the core duration of the flood-rich periods as the time differences between the centres of voxels, and we calculated the areas and volumes as the number of voxels included times their individual area and volume, respectively. As the interest of this study was in the large flood-rich periods, we only kept periods with volumes larger than 78711 km² yrs (corresponding to 10 voxels) for further analysis. This resulted in a total of 74 flood-rich periods for which the projected area (km²), the space-time extent or volume (km² yrs), a scaled space-time extent (0 for the smallest of the 74 events, 1 for the largest), and the scaled mean intensity of the period were calculated. The periods were ranked by the sum of the scaled space-time extent and scaled mean intensity. The top periods thus identified were 1756-1792 followed by 1840-1872 and 1992-2016. Changing the ranking function slightly changed the ordering of the periods, but the largest periods always remained at the top. The top ten periods were given Roman numerals in chronological order (Extended Data Table 2). Two periods (Va and Vb) were given a combined name due to their overlap in time. The results are moderately sensitive to the ratio parameter. For example, changing it from 50 to 100 and 25 km/yr, changes the extent of period IX from 1.8 to 2.3 and $1.2 \cdot 10^6$ km², the duration from 25 to 17 and 25 years, and the volume from 19 to 23 and $14 \cdot 10^6$ km² yrs, respectively. The positions in time and space of the centres of the periods change little in most cases, and the current top 8 events remain in the list of top 10 events. The results show little sensitivity to the choice of the smoothing and tapering range parameters of the spline interpolation.

Air temperatures

We used a 500-year Central European temperature reconstruction[14] to evaluate the air temperatures of the flood-rich periods, which we consider to currently be the highest quality reconstruction in Europe, as the annual correlations with other, more local, historical series in Europe are relatively high. The correlation coefficients with the series in Barcelona, Central England and Stockholm are 0.67, 0.73 and 0.64, respectively[59, 60, 61] which indicates spatial representativeness over much of Europe. The data are temperature deviations (anomalies) from the mean 1961-1990 and have been derived from documentary sources such as chronicles, weather diaries, accounts, letters, newspapers and legal sources. Potential biases and limitations may derive from data coverage and calibration relationships varying in time. We chose annual rather than seasonal temperatures for the analysis because we intended to not only capture flood event properties, but also antecedent soil moisture and snow conditions which can be relevant for flood magnitudes over more than one season. Annual and seasonal temperature averages over decades are correlated with r=0.75, 0.75 and 0.82 for summer, autumn and winter, respectively.

17

The average air temperatures of each flood-rich period were estimated separately for five regions in Europe, Eastern Europe (Russia, Latvia), Northern Europe (Sweden, Norway), Central Europe (Poland, Czechia, Hungary, Austria, Switzerland, Germany), Western Europe (Netherlands, Belgium, Great Britain, France), Southern Europe (Portugal, Spain, Italy) (Extended Data Fig. 1). Based on the spatial locations of the flood-rich periods, Eastern Europe showed some signal during period V (due to class 3 floods in 1760, 1761, 1770, 1771, 1777, 1779 and 1784 and 8 class 2 floods) and period VII (due to a class 3 flood in 1877 and 13 class 2 floods), however this was too weak to be included (possibly a result of lower data density). In Northern Europe, flood-rich periods Vb and VIII occurred, in Central Europe I, II, IV, Va, VII, IX, in Western Europe I, II, IV, Va, VI, IX, and in Southern Europe III, Va, VI, IX. Additionally, average temperatures were estimated for periods between these flood-rich periods (termed interflood periods here). The 90% confidence bounds of these averages m_T were estimated by $m_T \pm 1.645\sqrt{v_T / n}$ where v_T is the variance of the annual temperatures and n is the number of years in the period. Fig. 4b and Extended Data Fig. 4bd compare the average temperatures of the flood-rich periods with those of the interflood periods before and after (for period I only after, for period IX only before).

Seasonality analysis

The flood-rich periods were also analysed with respect to their average flood seasonality for the same five regions. In contrast to the interpolation of the intensities, for the seasonality all 103 series and all floods (including no. 1 floods) were included in order to develop a more robust estimate of seasonality, which tends to vary significantly between events[62]. Including the no. 1 classified floods reduced uncertainty in the flood seasonality resulting from missing data. The analysis was performed considering all flood events, i.e., in some cases more than one flood per year per site. As we were more interested in the seasonality of the large floods, while maintaining the robustness by including small events, we estimated the frequency of floods within each season as a weighted mean of the frequencies of each of the flood intensities, giving no. 1, 2, and 3 floods weights of 1, 2, and 3, respectively.

The lines in Fig. 5a and Extended Data Fig. 5ac show the frequency of floods in each season over the past 500 years applying a 30-year averaging window for Central, Southern and Western Europe. In Northern and Eastern Europe, the number of floods was too low to make reliable inferences on changes in seasonal flood frequencies. Fig. 5b and Extended Data Fig. 5bd show the averages of the frequencies over all interflood periods, the past flood-rich periods (excluding the recent one), and the recent flood-rich period IX. The 90% confidence bounds of the averages p_s were estimated by $p_s \pm 1.645\sqrt{p_s(1-p_s)/n}$, where n is the number of years with floods whose season is known.

Data Availability

The flood index data that were used in this paper and an extended list of references are available at https://github.com/tuwhydro/500yrfloods. The air temperature data are available at https://www.ncdc.noaa.gov/paleo-search/study/9970

Code availability

The data analysis was performed in R using the supporting package *fields* for the Thin Plate Spline interpolation (function *fastTps*). The code used can be downloaded from https://github.com/tuwhydro/500yrfloods.

Methods References

18

611[49] Brázdil, R. et al. Historical floods in Europe in the past Millennium. In: *Changes in Flood Risk in* 612*Europe* (ed Kundzewicz, Z.W.) (Wallingford IAHS Press, 2012), 121–166.

613[50] Sturm, K. et al. Floods in Central Europe since AD 1500 and their relation to the atmospheric 614circulation. *Petermanns Geogr. Mitt.* **145**, 14–23 (2001).

615[51] Salinas, J.L., Kiss, A. Viglione, Viertl, R., & Blöschl. G. A fuzzy Bayesian approach to flood frequency 616estimation with imprecise historical information. *Wat. Resour. Res.* **52**, 6730–6750 (20 16).

617[52] Kiss, A. *Floods and long-term water-level changes in medieval Hungary* (Cham Springer, 2019), 618280–285.[53] Viglione, A., Merz, B., Viet Dung, N., Parajka, J., Nester, T. & Blöschl, G. Attribution of 619regional flood changes based on scaling fingerprints. *Wat. Resour. Res.* **52**, 5322-5340 (2016).

620[54] Hall, J., et al. Understanding flood regime changes in Europe: a state of the art assessment. *Hydrol.* 621*Earth Syst. Sci.* **18**, 2735–2772 (2014).

622[55] Rogger, M. et al. Land-use change impacts on floods at the catchment scale - Challenges and 623opportunities for future research. *Wat. Resour. Res.* **53**, 5209–5219 (2017).

624[56] Rohr, C. *Extreme Naturereignisse im Ostalpenraum. Naturerfahrung im Spätmittelalter und am* 625*Beginn der Neuzeit* (Köln Böhlau, 2007), 558–562.

626[57] Skøien, J. & Blöschl, G. Catchments as space-time filters – a joint spatio-temporal geostatistical 627analysis of runoff and precipitation. *Hydrol. Earth Syst. Sci.* **10**, 645–662 (2006).

628[58] Haslinger, K. & Blöschl, G. Space-time patterns of meteorological drought events in the European 629Greater Alpine Region over the past 210 years. *Wat. Resour. Res.* **53**, 9807–9823 (2017).

630[59] Prohom, M., Barriendos, M. & Sanchez-Lorenzo, A. Reconstruction and homogenization of the 631longest instrumental precipitation series in the Iberian Peninsula (Barcelona, 1786-2014). *Int. J.* 632*Climatol.* **36**, 3072–3087 (2015).

633[60] Parker, D.E & Horton, E.B. Uncertainties in the Central England Temperature series since 1878 and 634some changes to the maximum and minimum series. *Int. J. Climatol.* **25**, 1173– 1188 (2005).

635[61] Moberg, A., Bergström, H., Ruiz Krigsman, J., & Svanered, O. Daily air temperature and pressure 636series for Stockholm (1756-1998). *Clim. Change* **53**, 171–212 (2002).

637[62] Hall, J. & Blöschl, G. Spatial patterns and characteristics of flood seasonality in Europe. *Hydrol.* 638*Earth Syst. Sci.* **22**, 3883-3901 (2018).

639[63] Nezhikovskij, R.A. *Reka Neva I Nevskaja Guba* (Leningrad Gidrometeoizdat, 1981), 81–84.

640[64] Mudelsee M., Deutsch, M., Börngen, M., & Tetzlaff, G. Trends in flood risk of the River Werra 641(Germany) over the past 500 years. *Hydrolog. Sci. J.*, **51**, 818–833 (2006).

642[65] Coeur, D. *La plaine de Grenoble face aux inondations* (Versailles Quae, 2004).

643

644

EXTENDED DATA FIGURES AND TABLES

Extended Data Fig. 1: Locations of the flood series. Series indicated by red circles are used for the interpolation of the flood intensities (names as in Extended Data Table 1 and Extended Data Fig. 2). Series indicated by orange circles are supplementary and only used for the seasonality analysis. Thick grey lines indicate regions used in the analysis.

20

Extended Data Table 1: Flood series, data contributors and countries, involved in the present study. Italics indicate the series only used for the seasonality analysis (denoted 'supplementary' in Extended Data Fig. 1). The code of the series (first column) consists of the country code and a running number.

Code of series	Country	Series provider/publication	River flood series	Catchment areas (1000 km²)
RU01, RU03-RU05	Russia (1)	Andrei Panin	Dnieper, Severnaya Dvina, Upper Volga, Lower Volga	504, 357, 236, 1380
RU02	Russia (2)	Published [63]	Neva	281
LV01	Latvia	Andrei Panin	Daugava	88
SE01-SE04	Sweden	Dag Retsö	Dalalven, Gota alv, Motala strom, Norrstrom	29, 50, 15, 23
NO01-NO10	Norway	Lars Roald	Driva, Gaula, Glomma, Numedalslagen, Olden, Orkla, Skienselv, Tinne, Valldola, Vosso	2.5, 3.7, 41, 56, 0.6, 3.1, 11, 0.2, 1.1, 1.5
PL01-PL02	Poland	Radoslav Doctor	*Upper Odra*, Vistula	106, 51
CZ01-CZ05, CZ08	Czech Republic (1)	Rudolf Brázdil	Dyje, Elbe, Morava, Middle Odra, Ohře, Vltava	11, 51, 21, 7.2, 113, 4.6, 28
CZ06-CZ07	Czech Republic (2)	Líbor Elleder	Lower Otava, *Upper Otava*	2.9, 0.5
HU01-HU03	Hungary	Andrea Kiss	Middle Danube, Maros, Tisza	210, 27, 157
HR01	Croatia	Hrvoje Petrić	Drava	40
AT01	Austria (1)	Christian Rohr	Traun	4.1
AT02	Austria (2)	Partly published; compiled and indexed: Andrea Kiss	Wien	0.2
CH02, CH04, CH06-CH11	Switzerland (1)	Petra Schmocker-Fackel	*Alpenrhein*, *Emme*, Muotha, *Schächen*, *Sihl*, *Sitter*, *Thur*, *Umäsch*	6.2, 0.4, 0.3, 0.1, 0.3, 0.3, 1.7, 0.07
CH01	Switzerland (2)	Oliver Wetter	Upper Rhine	30
CH03, CH05	Switzerland (3)	Lothar Schulte	Aare, *Lutschine*	0.03, 0.4
DE05-DE06	Germany (1)	Rüdiger Glaser, Johannes Schönbeim	Main, Upper Danube	27, 7.5
DE01-DE04, DE07	Germany (2)	Oliver Böhm	Inn, *Iller*, Isar, Lech, *Salzach*	12, 1.0, 4.1, 3.9, 6.6
DE08	Germany (3)	Published [64]	Werra	5.5
NL01	Netherlands	Willem H.J. Toonen	Lower Rhine	185
BE01-BE04	Belgium	Gaston Demaree	Jeker, *Hoyoux*, Sambre, Meuse	0.5, 0.3, 2.7, 36
GB01-GB03	United Kingdom	Neil Macdonald	Yorkshire Ouse, Tay, Trent	3.3, 4.6, 7.5
FR01-FR02, FR04-FR05, FR07-FR015	France (1)	Denis Coeur	Allier, Durance, Middle Garonne, Upper Garonne, *Middle Loire*, Lower Loire, Marne, Oise, Rhône, Saone, Seine, Tarn, Yonne	14, 14, 52, 14, 39, 117, 13, 17, 96, 30, 44, 9.7, 11
FR03, FR06	France (2)	Published [65]	Drac, Isere	3.6, 9.5
PT01	Portugal	Inês Amorim, João Carlos Garcia, Luís Pedro Silva	Lower Duero	98
ES01-ES16, ES18-ES20	Spain (1)	Mariano Barriendos	Middle Duero, Lower Ebro, Upper Ebro, Guadalmedina, Guadalquivir, Jucar, Llobregat, Nervion, *Pisuerga*, Rieres Pla de Barcelona, Sa Riera Mallorca, *Upper Segre*, *Middle Segre*, Lower Segre, Segura, R. Sobirans, Tajo, Ter, Turia	40, 79, 15, 0.2, 57, 22, 4.9, 1.9, 15, 0.1, 0.1, 1.2, 1.7, 20, 20, 0.03, 82, 1.8, 6.4
ES17	Spain (2)	Gerardo Benito	Tagus	9.3
IT01-IT04	Italy	Silvia Enzi, Dario Camuffo, Chiara Bertolin	Adige, Arno, Po, Tiber	12, 8.2, 74, 17

21

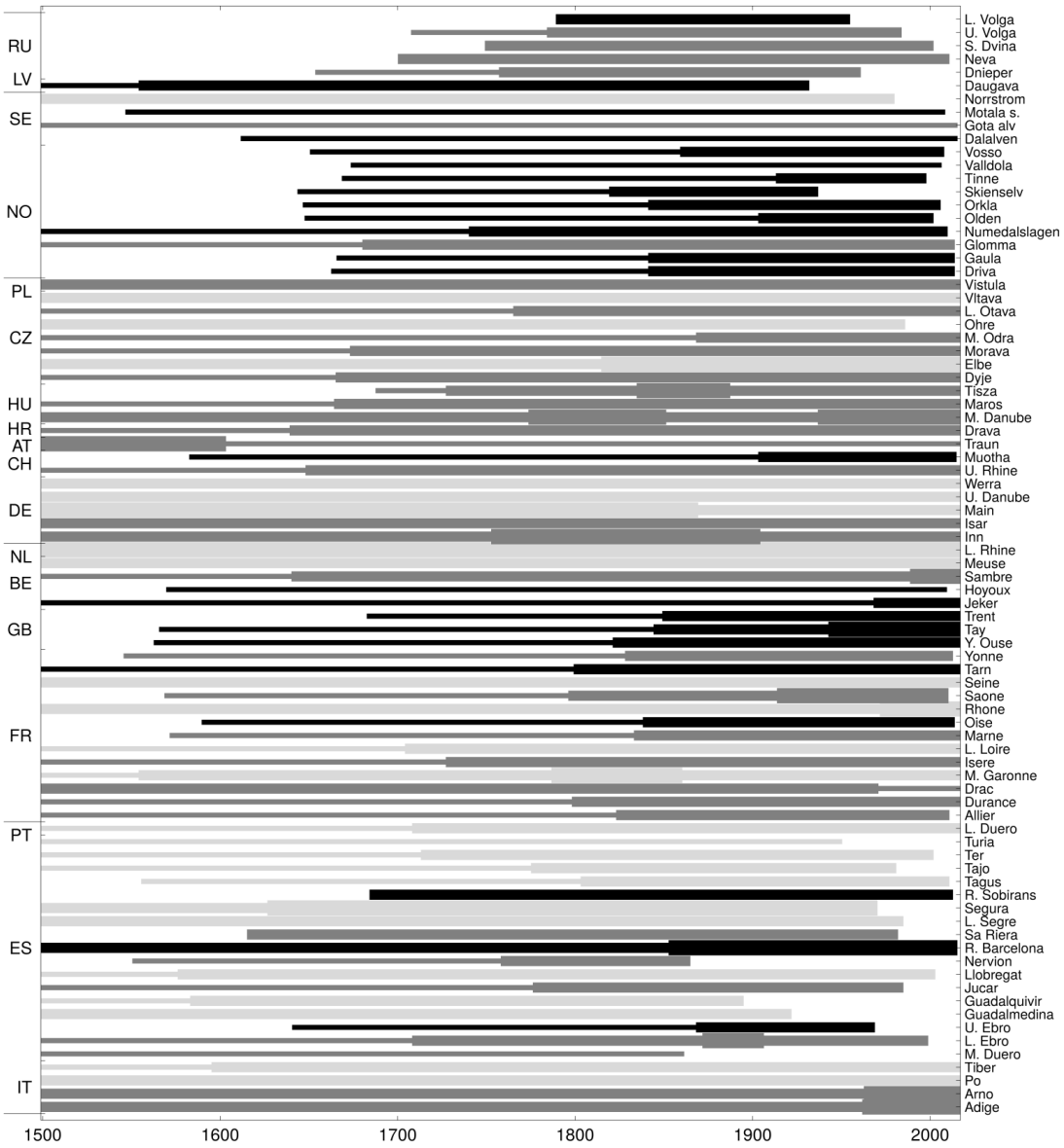

Extended Data Fig. 2: Duration, representativeness index and bias index of the flood data series. The grey scale refers to the representativeness index that reflects the degree of data representativeness in a regional context (light grey: low representativeness (u=1); dark grey: average representativeness (u=2); black: high representativeness (u=3). The line width refers to the bias index that reflects the completeness of the source material in a historical context (no line: no data; thin line: period with possibly missing data; average line: average; thick line: period with overly dense data.

22

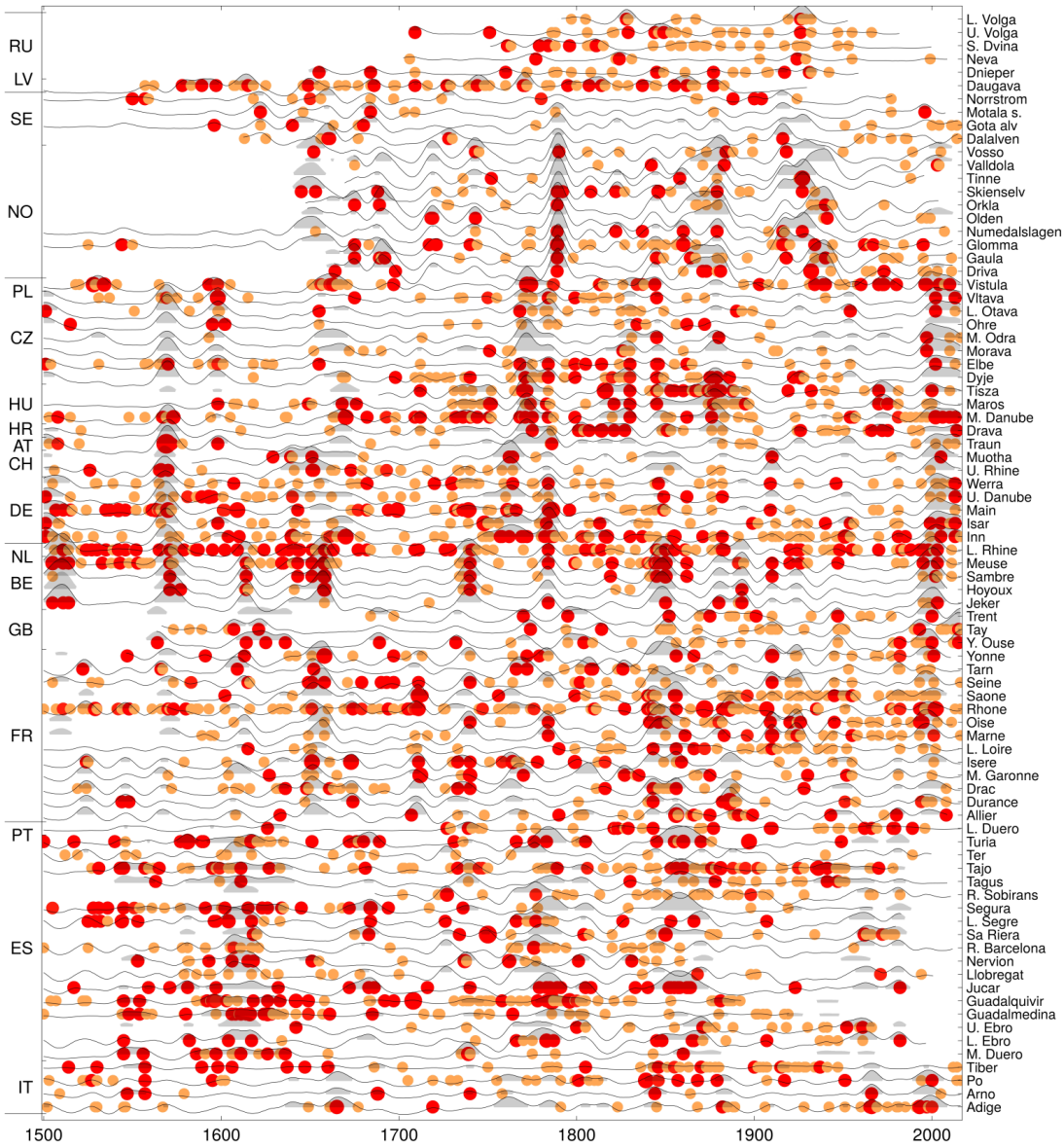

Extended Data Fig. 3: Raw data of flood intensities. Great (no. 2) and extraordinary (no. 3) floods are marked by orange and red dots, respectively. Thin lines show the interpolated flood intensities. Flood-rich periods are shown as light grey areas.

23

Extended Data Table 2: Flood-rich periods in Europe in the past 500 years. Full time periods obtained by generalising the core time periods, core time periods resulting from the analysis, durations of the core periods, regions, maximum area, volume (i.e. space-time domain covered by period), scaled volume, scaled mean intensity of the interpolated flood intensity, and rank. Scaling is from 0 to 1 for the 74 periods identified.

Period	Full time period	Core time period	Core duration (yrs)	Regions	Max area (10^6km^2)	Volume (10^6km^2 yrs)	Scaled volume	Scaled mean intensity	Rank
I	1500-1520	1500-1516	17	Western Europe, Central Europe	0.569	5.97	0.282	0.622	9
II	1560-1580	1564-1576	13	Western Europe, Central Europe	0.923	8.76	0.416	0.826	4
III	1590-1640	1592-1636	45	Iberia, Southern France	1.025	18.08	0.864	0.269	6
IV	1630-1660	1636-1660	25	Western Europe, West-Central Europe, Northern Italy	0.891	9.71	0.462	0.602	7
Va	1750-1800	1756-1792	37	Central Europe, Western Europe	1.830	20.92	1.000	0.627	1
Vb	1750-1800	1788-1792	5	Scandinavia	0.496	3.75	0.176	1.000	5
VI	1840-1880	1840-1872	33	Western Europe, Southern Europe	1.621	19.86	0.949	0.637	2
VII	1860-1900	1864-1892	29	East Central Europe	0.411	5.62	0.266	0.657	8
VIII	1910-1940	1916-1940	25	Scandinavia	0.573	5.71	0.270	0.627	10
IX	1990-2016	1992-2016	25	Western Europe, Central Europe, Italy	1.771	18.69	0.893	0.607	3

24

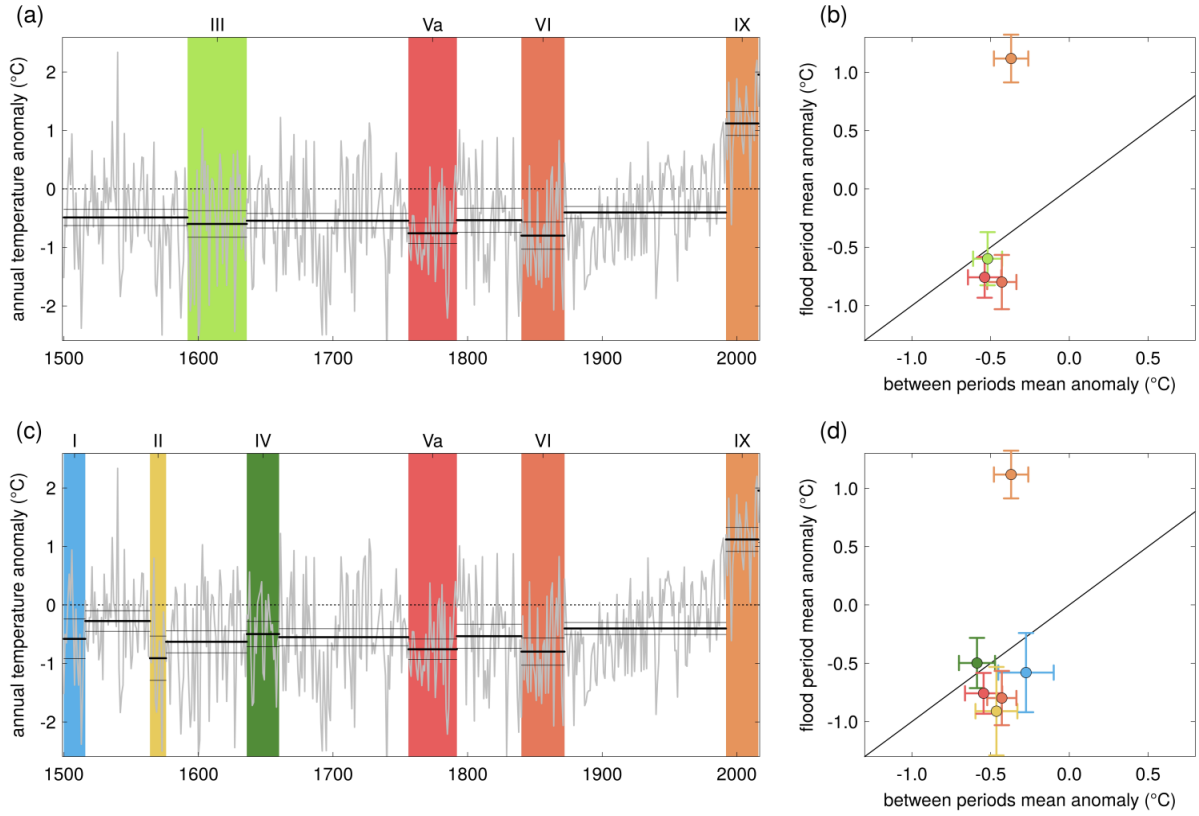

Extended Data Fig. 4: Anomalies of annual air temperatures from their 1961-1990 mean within and outside flood-rich periods in Southern Europe (top) and Western Europe (bottom). (a, c) Time series of air temperature anomalies (grey line) and their averages and 90% confidence bounds (black lines), and flood-rich periods indicated by colour bars. (b, d) Relationship between mean temperature anomalies in flood-rich periods and those of the intervals in between. Error bars show 90% confidence bounds. Colours correspond to those of the flood-rich periods in (a, c).

25

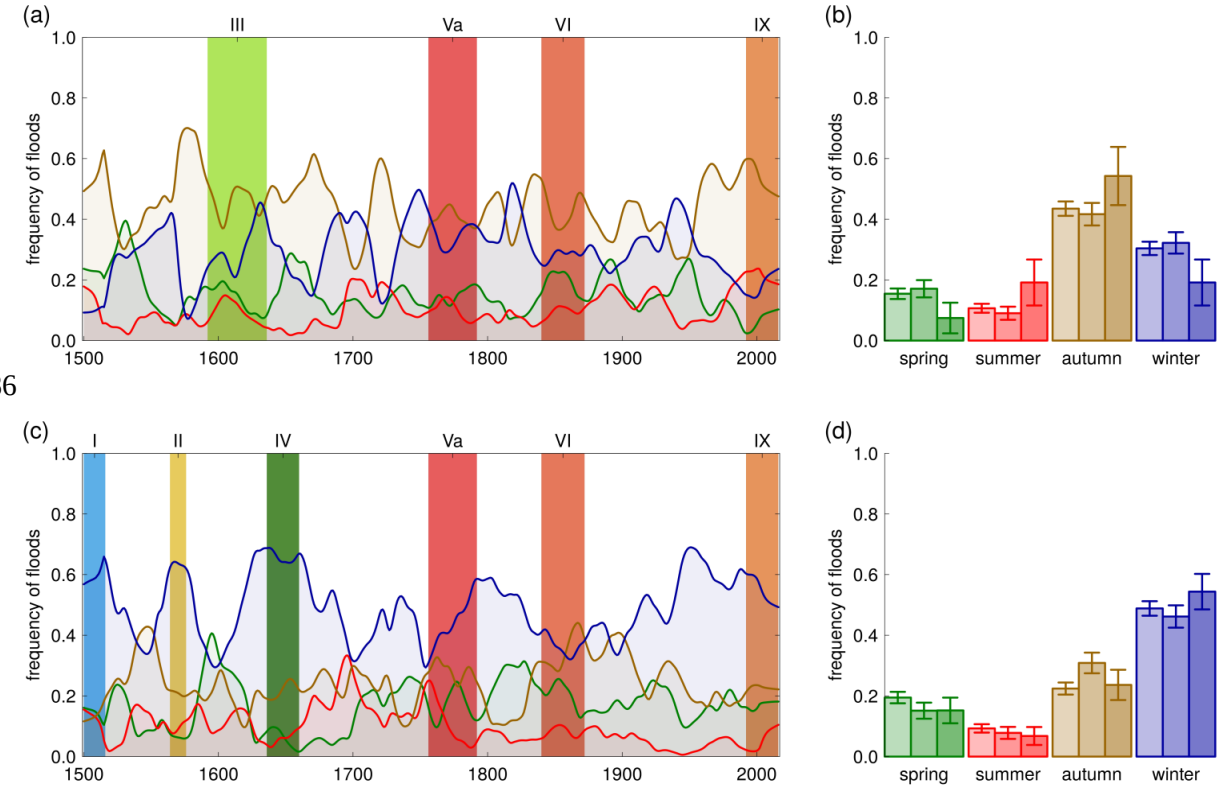

Extended Data Fig. 5: Seasonality of floods within and outside flood-rich periods in Southern Europe (top) and Western Europe (bottom). (a, c) Time series of smoothed frequency of floods in four seasons (lines, green: spring, red: summer, brown: autumn, blue: winter) and flood-rich periods indicated by colour bars. (b, d) Frequency of floods in four seasons. Left bars: interflood periods; middle bars: flood-rich periods of the past; right bars: flood-rich period IX (1990-2016). Error bars show 90% confidence bounds.

Supplementary information

Video 1: Dynamic visualisation of the flood-rich periods in Europe in the past 500 years and their relationship to air temperature.

26